

## The 'Extinction Curve' in the Investigation of the Optical Indicatrix

BY N. JOEL\* AND ISABEL GARAYOCHEA†

Laboratorio de Cristalografía, Facultad de Filosofía, Universidad de Chile, Casilla 147, Santiago, Chile

(Received 10 August 1956 and in revised form 12 February 1957)

A method is given for determining the orientation of the optical indicatrix of microscopic crystals directly from the 'extinction curve', which is obtained by means of a very convenient one-axis stage goniometer.

The three axes of the indicatrix appear on the projection of the extinction curve as three points  $X$ ,  $Y$ ,  $Z$ , which form a 'triangle'. The geometrical determination of this triangle leads in general to two solutions: the 'true triangle' and a 'ghost triangle'. The latter has some special properties by which it may be distinguished from the 'true triangle', and thus the three axes of the ellipsoid may be determined. Each of the three axes can then be identified.

The possibility of the method was first studied by means of a graphical survey of numerous typical cases. Accuracy tests and a brief mathematical treatment of the problem are also given.

*Resumen en Español.*—En este trabajo se da un método para determinar la orientación de la indicatriz óptica de cristales microscópicos directamente a partir de la 'curva de extinción', haciendo uso de un pequeño goniómetro de platina muy conveniente.

Los tres ejes de la indicatriz aparecen en la proyección de la curva de extinción como tres puntos  $X$ ,  $Y$  y  $Z$  que forman un 'triángulo'. La determinación geométrica de este triángulo conduce en general a dos soluciones: el 'triángulo verdadero' y un 'triángulo fantasma'. Este último tiene algunas propiedades especiales que permiten su identificación, y por consiguiente, la determinación de los tres ejes del elipsoide. A continuación, cada uno de los tres ejes puede ser identificado.

La posibilidad del método fué analizada primero a través de un estudio gráfico de numerosos casos típicos. Se da también algunas pruebas sobre la precisión del método y un breve tratamiento matemático del problema.

### 1. Introduction

The optical investigation by means of the polarizing microscope of small single crystals which are to be set afterwards in a diffraction camera for X-ray crystallographic work is greatly facilitated by the use of a one-axis stage goniometer, such as the one designed by Bernal & Carlisle (1947). This instrument is used with its axis perpendicular to the microscope axis, and parallel to the vibrations transmitted by the polarizer. The crystal is stuck with shellac (or any other similar adhesive) to a thin glass fibre, which is in turn fastened to the end of the goniometer axis with something like plasticine.

With the help of this very convenient instrument a method was developed for determining the optical indicatrix of small single crystals (Joel, 1950, 1951). The method is based on the 'extinction curve' of the crystal mounted on the goniometer. The extinction curve is the locus—in the stereogram—of the extinction directions of the crystal when the latter is rotated about an arbitrary but fixed axis, which is set perpendicular to the microscope axis.

A description of the extinction curve is given in § 2, especially in paragraphs (i) and (ii).

The experimental determination of the extinction curve for one particular setting is done by reading the positions  $\theta_1$  and  $\theta_2$  of the microscope stage which give extinction of the crystal between crossed nicols, for different positions  $\varphi$  of the stage goniometer, e.g. every  $10^\circ$ .

These readings can be put into a stereographic projection as shown in Fig. 3(c) and thus the extinction curve is obtained (see also paragraph (a) of § 3). It was also shown that this curve contains the points which represent the  $X$ ,  $Y$  and  $Z$  axes of the ellipsoid, and it was indicated how these three axes could be determined by finding in the crystal the direction of maximum or minimum refractive index.

The shape of the extinction curve for a given rotation axis also shows the way in which the crystal selects the two sets of vibration directions associated with that particular setting.

Further investigation of this subject showed that there are a number of interesting facts about these extinction curves worthy of mention, as well as some improvements in the method of studying the indicatrix. This applies particularly to those cases in which good interference figures cannot be observed.

\* Now at the Crystallographic Laboratory, Cavendish Laboratory, Cambridge, England.

† Now Mrs I. Wittke.

The validity of the new method is discussed in §§ 2, 4 and 5; but all the experimental details are given in § 3.

In this paper reference is made to biaxial crystals, since the problem of determining the orientation of the indicatrix of uniaxial crystals directly from the extinction curve has already been solved (Joel, 1950).

## 2. On the possibility of determining the orientation of the indicatrix directly from the extinction curves

The problem of locating the three points  $X$ ,  $Y$  and  $Z$  on the extinction curve may be stated in a geometrical form as follows: to determine on the extinction curve three points such that they should all be at an angular distance of  $90^\circ$  from each other. This set of three points will be referred to in this paper as the 'triangle'. If it could be shown that there is only one such triangle—apart from the obvious repetitions due to symmetry and orthogonality—it would appear very easy to determine it graphically, either on the stereographic projection, or on a sphere. This would mean that the orientation of the three axes of the indicatrix had been found.

Unfortunately, the equations that would lead to the determination of the triangle (or triangles) are extremely complicated. We tried to solve the problem using Euler angles, and obtained a set of three equations of the ninth degree. With Cartesian coordinates we obtained a set of six algebraic equations involving six unknowns, three of them of the third degree and the other three of the second degree.

It was clear to us that there was no hope in this direction, but we noticed that the number of solutions would have to be finite. And as to the real solutions, they might be few in number.

The problem was therefore tackled graphically, and it was decided to draw the extinction curve for different crystals and in each of them for different settings on the goniometer.

It was shown in the 1951 paper that if the curves of constant refractive index—called equivibration curves by Wright (1923) and Phemister (1954)—of a crystal are drawn at regular intervals radially projected on to a unit sphere, and if the direction of the goniometer axis be indicated by a point  $P_0$  on this sphere, the extinction curve is the locus of the points at which the great circles through  $P_0$  are tangent to the curves of constant refractive index. We would like to state now that it is not necessary to draw these curves of constant refractive index, either on a sphere or in a projection, if use is made of the Biot-Fresnel construction in the following way:

Consider a plane wave which travels through a crystal in any given direction: draw the diametral plane of the indicatrix parallel to the wave front; this plane is intersected by the two circular sections of the indicatrix along two lines, and the angles formed

by these two lines are bisected by the two vibration directions associated with the given wave normal.

Therefore it was sufficient to draw in the stereographic projection the two circular sections of the crystal and the point  $P_0$  (Fig. 1). On a set of great

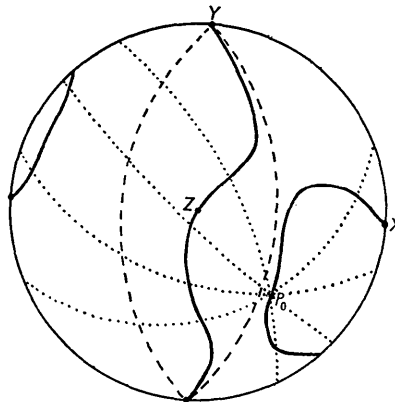


Fig. 1. The way the extinction curves were drawn. Broken lines: circular sections. Dotted lines: great circles through  $P_0$ . On these circles the points which are half-way between the circular sections are marked; the locus of these points is the extinction curve. In this diagram the curve through  $Y$  and  $Z$  is the equatorial curve, and the one through  $X$  and  $P_0$  is the polar curve. (Only the upper half is shown in the projections of Figs. 1-5.)

circles through  $P_0$ , taken at convenient intervals, the two points which are half way between the circular sections were marked; and in this way the extinction curve for that particular position of  $P_0$  relative to the indicatrix was obtained. Thus, an extinction curve will depend only on the optical angle  $2V$  of the crystal and the direction of the goniometer axis relative to the two circular sections (or the two optic axes) of the crystal.

Drawings were made for  $2V_\gamma = 90^\circ$ , and  $2V_\gamma = 46^\circ$  (positive)—which obviously also accounts for  $2V_\gamma = 134^\circ$  (negative). In the actual experimental procedure, the goniometer axis always lies in the plane of the microscope stage; that is,  $P_0$  is always on the projection circle, while the points  $X$ ,  $Y$  and  $Z$  have any position—mutually perpendicular, of course. In our drawings, on the other hand, it proved much more convenient to keep points  $X$  and  $Y$  on the projection circle—which will project  $Z$  on the centre of this circle—and to move the point  $P_0$  about in some regular manner so as to cover all typical cases.

For each position of  $P_0$  the extinction curve consists of:

(i) A curve that runs round the sphere and which is itself centrosymmetric; this will be called the 'equatorial curve', although it may differ considerably from a great circle.

(ii) A set of two smaller curves—their largest angular diameter never exceeds  $90^\circ$ —which are mutually symmetric relative to the centre of the sphere; these will be called 'polar curves' (Fig. 1).

There are some interesting features of the extinction curves, which will be useful at a later stage and which are a consequence of the well known fact that the refractive indices associated with the vibration directions permitted by the crystal on rotation about its axis fall into two groups: one limited to the range  $\alpha$  to  $\beta$ , and the other to the range  $\beta$  to  $\gamma$ ; furthermore, one of these ranges is always fully covered, while the other does not in fact necessarily reach the  $\beta$  end of the interval.

These features are: first, the extinction curve does not go through the circular sections, except at their two common points  $Y$  and  $\bar{Y}$ , and, if we consider the dihedral angles formed by the two circular sections, the polar curves are confined to the two dihedrals (one in each) which contain  $P_0$ , while the equatorial curve is confined to the other two; secondly, of the three points  $X$ ,  $Y$  and  $Z$ , two are on the equatorial curve and one on the polar curve; and thirdly, the point  $Y$  is always on the equatorial curve and the point  $P_0$  is always on the polar curve.

A limiting case arises when  $P_0$  is on a circular section of the crystal (in other words, when the plane perpendicular to the rotation axis  $P_0$  contains one of the optic axes of the crystal): the equatorial curve and the two polar curves join at four singular points which are on the same circular section; the extinction curve includes this circular section, in such a way that one half of the latter is covered by the equatorial curve and the other half by the polar curves.

As the extinction curves are centrosymmetric, in all the diagrams (Figs. 1-5) only the upper half is drawn. Therefore, there is only half of the equatorial curve, and parts of the polar curves which together correspond to one of them. It is quite easy to imagine the remainder of the extinction curve. This will simplify the figures, as in some of them several positions of  $P_0$  are shown in each drawing, with as many extinction curves (half an equatorial curve and

one polar curve for each). In other cases, the equatorial curve may appear broken in several parts.

For each of the values of  $2V_\gamma$ , considered in this graphical survey, the extinction curve for about 60 different positions of  $P_0$  were drawn out; Fig. 2 shows some typical examples.

Many of these curves were then transferred to a sphere, which was quite easy, with two main purposes:

(1) To see whether at the points  $X$ ,  $Y$  and  $Z$  the extinction curves had any special geometrical properties, especially with regard to curvature or torsion, which might lead to their determination on the experimentally-obtained extinction curve. This analysis is not possible in the projection owing to its distortion. This idea proved unsuccessful, so we proceeded to the second one:

(2) To see how many triangles as defined above can be located on each of the extinction curves. This was done on the sphere by means of a spherical triangle with its three angles of  $90^\circ$ , made out of wire thick enough to keep its shape. The sides of this wire triangle had the same radius as the sphere.

As all triangles that might exist have two vertices on the equatorial curve and one on the polar curve, the wire triangle was moved on the sphere, keeping two of its vertices on the equatorial curve and drawing at the same time the locus of the third vertex. This procedure showed that there are three different cases:

(a)  $P_0$  is not on any of the three principal planes of the indicatrix. This is the general case. There are two triangles: one is actually the set of points  $XYZ$ , and will be called the 'true triangle'; and another one, which is obviously not the solution of our problem, and which will be called the 'ghost triangle'.

(b)  $P_0$  is on any of the three principal planes of the indicatrix. In this case the extinction curve is symmetric relative to the principal plane of the indicatrix which contains  $P_0$ ; only one triangle is found, and it is the true one. Actually what happens is that when

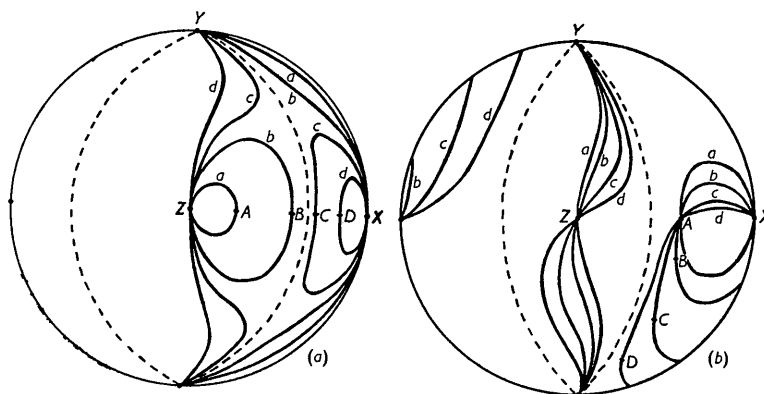


Fig. 2. (a) Some extinction curves for  $2V_\gamma = 46^\circ$  (or  $134^\circ$ ). Broken lines: circular sections.  $A$ ,  $B$ ,  $C$  and  $D$  are four different positions of  $P_0$  in the plane  $XZ$ , and therefore the corresponding extinction curves,  $a$ ,  $b$ ,  $c$  and  $d$ , are symmetric relative to this plane. (b) Some extinction curves for  $2V_\gamma = 90^\circ$ . Broken lines: circular sections.  $A$ ,  $B$ ,  $C$  and  $D$  are four different positions of  $P_0$ , and  $a$ ,  $b$ ,  $c$  and  $d$  are the corresponding extinction curves.

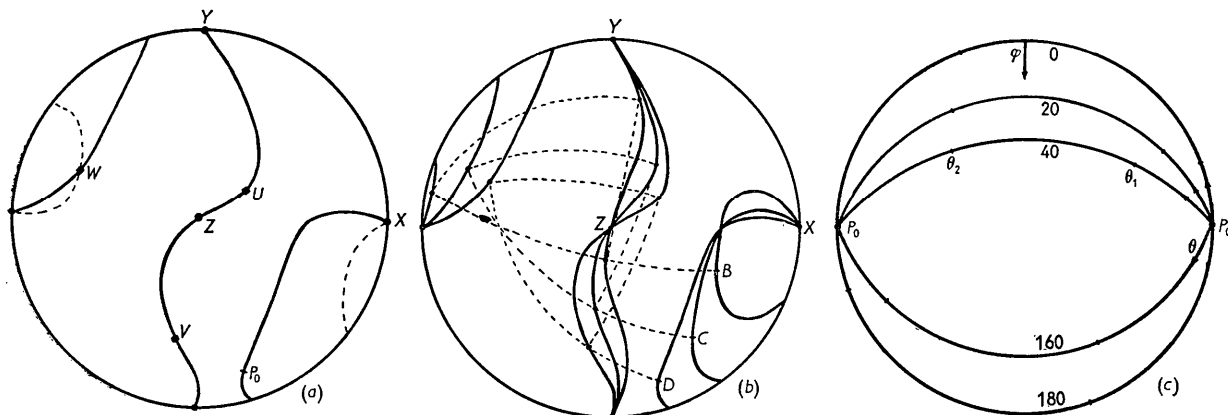


Fig. 3. (a) An extinction curve with the locus (broken line) of the third vertex of a 'triangle' while the other two move on the equatorial curve.  $U$ ,  $V$  and  $W$  are the vertices of the 'ghost triangle';  $X$ ,  $Y$  and  $Z$  are the vertices of the 'true triangle'. (b) Three of the extinction curves of Fig. 2(b), each with its ghost triangle (broken lines), one side of which passes through  $B$ ,  $C$  and  $D$  respectively. ( $B$ ,  $C$  and  $D$  are the positions of  $P_0$  corresponding to the curves shown.) (c) The plotting of the extinction directions with the one-axis stage goniometer.  $P_0$  is the goniometer axis. The numbers on the great circles through  $P_0$  are the corresponding values of  $\varphi$  (goniometer readings), and the dots on them are the extinction directions (vibration directions) given by the readings  $\theta_1$  and  $\theta_2$  on the microscope stage.

$P_0$  approaches one of the principal planes of the indicatrix, the ghost triangle tends to coincide with the true triangle.

(c)  $P_0$  coincides with one of the three axes of the indicatrix. In this particular case an infinite number of triangles is found, as the polar curve is reduced to the point  $P_0$  (which is one of the three axes of the indicatrix), and the equatorial curve becomes a great circle perpendicular to  $P_0$ .

The operation of drawing the locus of the third vertex of the triangle while the other two move on the equatorial curve was then performed for many typical cases in the stereographic projection; this is more accurate than doing it on the sphere, but takes more time as the triangle does not keep its shape and size in the projection while it moves on the sphere. Fig. 3(a) shows a drawing of an extinction curve, with its locus for the third vertex of the triangle.

We will refer now to the general case. Although it could not be proved mathematically, the analysis of our many drawings had led to the indubitable conclusion that there are no more than two triangles. But, for this method to be of any use, it would be necessary to find a way to decide which of the two triangles thus determined on the experimental extinction curve is the true one. Close inspection of the drawings showed a very surprising fact: in all of them the ghost triangle seemed to have one of its vertices  $90^\circ$  away from  $P_0$ . Or, in other words,  $P_0$  always lies on one side of the ghost triangle (Fig. 3(b)). This could, in fact, be proved (see § 5.2), and constitutes, therefore, the required means of identifying the ghost triangle.

### 3. Experimental procedure

(a) The crystal is mounted on the one-axis stage goniometer, and the extinction curve for that partic-

ular setting is plotted on a stereographic projection in the way described in the 1950 paper and reviewed in § 1 of the present paper. Fig. 3(c) indicates the plotting of the points for a goniometer showing increasing readings when turned away from the observer, and for a rotating microscope stage showing increasing readings when turned clockwise (numbered anticlockwise). The letters  $\theta$  and  $\varphi$  are here interchanged, as compared to their use in the 1950 and 1951 papers, in order to conform to the usual nomenclature in analytical geometry. The numbers on the great circles are the corresponding values of  $\varphi$  (readings on the goniometer), and the dots on them are the extinction directions (vibration directions) as obtained through the readings of  $\theta$  on the microscope stage.

There are two sets of points (extinction directions), one for  $\theta_1$  and the other for  $\theta_2$ . One of these sets of points will give the equatorial curve, and the other set will give the polar curve; and these two curves constitute the extinction curve for that particular setting of the crystal.

During the reading of the extinction directions the crystal should be immersed in a drop of liquid of refractive index approximately equal to the average index of the crystal; this is easy to achieve on the one-axis stage goniometer.

(b) The next step is the determination of the three axes of the indicatrix, in other words, the true triangle. Two of its vertices lie on the equatorial curve; therefore two points of the latter which are  $90^\circ$  apart are chosen, and the pole of the great circle that passes through them is plotted. By repeating this for several such pairs of points, taken in turn, the locus of the third vertex of the triangle is obtained (Figs. 3(a) and 5). This locus intersects the polar curve at two points, thus determining the two triangles. In order to know which is the 'true' one and which is the

'ghost' one, it is sufficient to remember that one of the vertices of the ghost triangle is  $90^\circ$  away from  $P_0$  (the goniometer axis). In fact, the ghost triangle can be found immediately after having plotted the extinction curve: determine the point  $U$  of the equatorial curve which is  $90^\circ$  away from  $P_0$  and draw the great circle of which  $U$  is the pole; this circle will intersect the extinction curve at the points  $V$  and  $W$ .  $U$ ,  $V$  and  $W$  are the vertices of the ghost triangle.

If the extinction curve has a plane of symmetry, which means that  $P_0$  is in one of the three principal planes of the indicatrix, the solution is immediate, for in this case the two triangles coincide and their location is determined in the straightforward manner described in the last paragraph for the ghost triangle.

If the equatorial curve is a great circle, the polar curve is reduced to the point  $P_0$ . The latter is in this case one of the axes of the indicatrix; and the other two cannot be determined geometrically but only through measurements of refractive indices at points along the equatorial curve. There is hardly the need to add that the occurrence of this particular case has an extremely small probability, unless one actually tried to obtain it.

(c) As to the identification of the three axes, it is already known that  $Y$  is on the equatorial curve. To determine whether the axis on the polar curve is  $X$  or  $Z$ , use can be made of a compensator in the usual way (one-wavelength retardation plate, wedge, Berek compensator, etc.) making use of the fact that all points of the equatorial curve represent vibrations restricted to the range  $\alpha-\beta$  if it contains the  $X$  axis, or to the range  $\beta-\gamma$  if it contains the  $Z$  axis.

It remains to be decided which of the two axes contained in the equatorial curve is  $Y$ . This cannot in general be done with the compensator or by means of the interference colours, owing to the variable thickness of the crystal sections. But it may be attempted in one of the following ways:

(i) By means of the Becke-line effect.—If the liquid in which the crystal is immersed happens to have its refractive index between the two main refractive indices corresponding to the two axes contained in the equatorial curve, it is easy to find which of the two is the  $Y$  axis by observing the Becke-line effect in different positions of the goniometer. For instance, if  $X$  and  $Y$  are on the equatorial curve, then when  $X$  (or a point near it) is horizontal the refractive index of the crystal will be smaller than that of the liquid; when  $Y$  is horizontal the reverse will be true.

(ii) By trying to observe an interference figure.—Even with a poor interference figure, which by itself would have been insufficient to ascertain the orientation of the ellipsoid, it might be possible to decide now which of the two known directions belongs to the  $Y$  axis (perpendicular to the optic axial plane of the crystal) and which belongs to the other axis (either  $X$  or  $Z$ , bisectors of the angles formed by the optic axes).

(iii) By observing the shape of the extinction curve.—This may give a better clue the bigger the polar curve or the more the equatorial curve departs from a great circle. In fact, when  $P_0$  approaches a circular section, a good deal of the polar curve runs close to it as well, i.e. in the region of the polar curve around  $P_0$ ; and a part of the equatorial curve (two symmetric parts) also runs close to the same circular section. Therefore, an attempt to fit the two circular sections between the equatorial and the polar curves, both of them passing of course through  $Y$ , may in some cases decide which of the two axes on the equatorial curve is  $Y$ .

Thus, the three axes of the indicatrix have been located.

If also the three principal refractive indices have to be measured, this can be done by bringing in turn each of the three axes of the indicatrix into the plane of the microscope stage and using the well known Becke-line method. For this, and also for the test described in paragraph (i) of this § 3, it is necessary to know which of the two extinction directions corresponding to a given position of the goniometer is set parallel to the vibrations transmitted by the polarizer.

As a final remark on the advantage of this method for X-ray crystallography, we would like to add that it can also be used with the crystal already mounted on the holder of the diffraction camera, with the help of a vertical goniometric arrangement which allows the crystal to rotate in the liquid contained in a small glass cell. The observations can be carried out by means of a microscope such as the one attached to single-crystal diffraction cameras and a simple polarizing outfit such as the convenient Perutz polarizing attachment (Perutz, 1949) made by Unicam. With an arrangement such as this we have also been able to use this method on crystals of macroscopic size.

#### 4. Accuracy tests

The method described in this paper for determining the indicatrix was tried out by us on several biaxial crystals. The accuracy of the results depends on the particular setting of the crystal, as there are favourable and unfavourable settings.

One test on a triclinic crystal is shown in Fig. 4, where the theoretical extinction curve, drawn after the indicatrix had been determined, is compared with the experimental curve. More tests of this kind were carried out, with similar results, on other biaxial crystals such as aragonite, ammonium oxalate, sodium pyrophosphate and zinc sulphate.

More direct tests were also carried out, of which an example is shown in Fig. 5. A cleavage fragment of anhydrite (orthorhombic) with well developed pinacoidal cleavages was chosen. The positions of the axes of the indicatrix, as determined by the method under discussion, are compared with the poles of the

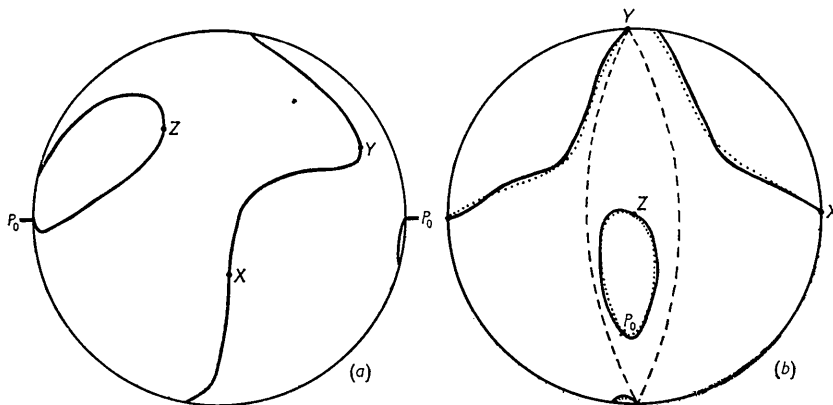


Fig. 4. (a) An experimental extinction curve for a crystal of  $\text{CuSO}_4 \cdot 5\text{H}_2\text{O}$  (triclinic); the orientation of the indicatrix was unknown.  $P_0$  is the position of the rotation axis.  $X$ ,  $Y$  and  $Z$  are the positions of the axes of the ellipsoid as determined from the extinction curve. (b) Full line: same experimental curve of (a), with the  $Z$  axis transferred to the centre of the projection, for comparison. Dotted line: theoretical extinction curve drawn after the relative positions of  $P_0$  and the indicatrix had been determined. Broken line: circular sections,  $2V_\gamma = 122^\circ$ .

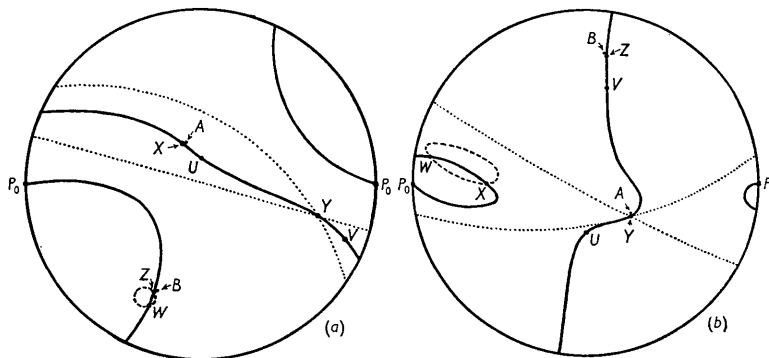


Fig. 5. (a) Anhydrite,  $\text{CaSO}_4$ , orthorhombic,  $2V_\gamma = 42^\circ$ . Extinction curve (full line), locus of the third vertex (broken line), ghost triangle  $UVW$ , and true triangle  $XYZ$ , as determined by the present method. Points  $A$  and  $B$  next to  $X$  and  $Z$  are the poles of pinacoids of the crystal; the errors in the directions of  $X$  and  $Z$  are about  $1^\circ$ . The two circular sections (dotted line) have been added. (b) Anhydrite, similar to (a) but with a different setting. The equatorial curve departs more from a great circle and the locus of the third vertex becomes in this case a larger curve, making the determination of  $XYZ$  more accurate. The errors on  $Y$  and  $Z$  are shown; they are less than  $1^\circ$ .

(In both (a) and (b) the errors appear exaggerated to avoid confusion.)

pinacoidal planes of the crystal: on symmetry requirements they should coincide; the experimental departure is about  $1^\circ$ . Fig. 5(b) corresponds to a more favourable setting of the crystal than Fig. 5(a): it can be seen that the locus of the third vertex of the triangle is a larger curve in Fig. 5(b); this means that the position of the third vertex is more sensitive to a displacement of the other two vertices along the equatorial curve. This depends, as can also be seen by comparison of these two figures, on how much the equatorial curve departs from a great circle.

## 5. Mathematical treatment

The mathematical definition of the extinction curve is the following: Let  $P_0$  be a point on the surface of an ellipsoid (the optical indicatrix) whose centre is  $O$ , and consider a diametral plane through  $OP_0$ . This

plane intersects the ellipsoid along an ellipse whose axes  $D_1$  and  $D_2$  pass through the surface of the ellipsoid at four points  $E_1, E'_1, E_2, E'_2$ . The locus of these points  $E$  when the diametral plane rotates round the line  $OP_0$  is the extinction curve. Defined in this way, the extinction curve lies on the ellipsoid; but, as has been said earlier, it is more convenient to project it radially on to a sphere of unit radius concentric with the ellipsoid.

We will follow the notation of Wilson's *Vector Analysis* (1943).

### 5.1. The equations of the extinction curves

The equation of the indicatrix (refractive index ellipsoid)

$$x^2/\alpha^2 + y^2/\beta^2 + z^2/\gamma^2 = 1$$

may be expressed by means of the dyadic

$$\Phi = \alpha^{-2}\mathbf{i}\mathbf{i} + \beta^{-2}\mathbf{j}\mathbf{j} + \gamma^{-2}\mathbf{k}\mathbf{k}$$

and the vector

$$\mathbf{r} = x\mathbf{i} + y\mathbf{j} + z\mathbf{k}$$

as follows:

$$\mathbf{r} \cdot \Phi \cdot \mathbf{r} = 1. \quad (1)$$

The cones of constant refractive index  $n$ :

$$\left(\frac{1}{\alpha^2} - \frac{1}{n^2}\right)x^2 + \left(\frac{1}{\beta^2} - \frac{1}{n^2}\right)y^2 + \left(\frac{1}{\gamma^2} - \frac{1}{n^2}\right)z^2 = 0$$

intersect the unit sphere, thus determining the curves of constant refractive index  $n$ . The equations of these curves are:

$$\mathbf{r} \cdot \Phi \cdot \mathbf{r} = n^{-2}, \quad \mathbf{r}^2 = 1. \quad (2)$$

Let  $\mathbf{r}_0$  be the vector drawn from the origin to the point  $P_0$  where the goniometer axis intersects the unit sphere. The equations of the great circle that passes through the fixed point  $P_0$  and another point  $P_1$ , which changes when the crystal turns round, are:

$$\mathbf{r} \cdot \mathbf{r}_0 \times \mathbf{r}_1 = 0, \quad \mathbf{r}^2 = 1. \quad (3)$$

The contact points of this great circle with two of the constant refractive index curves are given by:

$$\left. \begin{aligned} \mathbf{r} \cdot (\Phi \cdot \mathbf{r}) \times (\mathbf{r}_0 \times \mathbf{r}_1) &= 0, \\ \mathbf{r} \cdot \Phi \cdot \mathbf{r} &= n^{-2}, \\ \mathbf{r}^2 &= 1. \end{aligned} \right\} \quad (4)$$

The equations of the extinction curves are obtained by eliminating  $\mathbf{r}_1$  and  $n$  from equations (4):

$$(\mathbf{r} \cdot \Phi \cdot \mathbf{r})(\mathbf{r} \cdot \mathbf{r}_0) = \mathbf{r} \cdot \Phi \cdot \mathbf{r}_0, \quad \mathbf{r}^2 = 1. \quad (5)$$

Equations (5) may be written in Cartesian coordinates:

$$\left. \begin{aligned} \left(\frac{x^2}{\alpha^2} + \frac{y^2}{\beta^2} + \frac{z^2}{\gamma^2}\right)(x_0x + y_0y + z_0z) \\ = \frac{x_0x}{\alpha^2} + \frac{y_0y}{\beta^2} + \frac{z_0z}{\gamma^2}, \quad x^2 + y^2 + z^2 = 1. \end{aligned} \right\} \quad (5')$$

5.2. Proof of the existence of a 'ghost triangle' ( $U, V, W$ ) of which one vertex  $U$  is  $90^\circ$  away from  $P_0$

The equation of the plane normal to  $\mathbf{r}_0$  is

$$\mathbf{r} \cdot \mathbf{r}_0 = 0. \quad (6)$$

Equations (5) and (6) give the vector  $\mathbf{u}$  which goes from the origin to  $U$ :

$$\mathbf{u} = \frac{\mathbf{r}_0 \times \Phi \cdot \mathbf{r}_0}{|\mathbf{r}_0 \times \Phi \cdot \mathbf{r}_0|}. \quad (7)$$

The equation of the plane normal to  $\mathbf{u}$  is:

$$\mathbf{u} \cdot \mathbf{r} = 0 \quad (8)$$

or

$$\mathbf{r} \cdot \mathbf{r}_0 \times \Phi \cdot \mathbf{r}_0 = 0. \quad (8')$$

It follows from (8') that the vectors  $\mathbf{r}, \mathbf{r}_0$  and  $\Phi \cdot \mathbf{r}_0$  are coplanar. Hence, equation (8') may be written thus:

$$\mathbf{r} = \lambda_1 \mathbf{r}_0 + \lambda_2 \Phi \cdot \mathbf{r}_0. \quad (8'')$$

The points  $V$  and  $W$  are determined by equations (5) and (8''). By imposing the condition that  $\mathbf{r}$  must be a unit vector, (8'') may be written:

$$\mathbf{r} = \frac{\mathbf{r}_0 + \lambda \Phi \cdot \mathbf{r}_0}{\pm |\mathbf{r}_0 + \lambda \Phi \cdot \mathbf{r}_0|}, \quad (9)$$

where  $\lambda = \lambda_2/\lambda_1$ .

By introducing (9) in the first of equations (5), an equation of the second degree in  $\lambda$  is obtained:

$$t_2 \lambda^2 + t_1 \lambda + t_0 = 0, \quad (10)$$

where

$$\left. \begin{aligned} t_0 &= (\mathbf{r}_0 \cdot \Phi \cdot \mathbf{r}_0)^2 - (\Phi \cdot \mathbf{r}_0)^2, \\ t_1 &= (\Phi \cdot \mathbf{r}_0)^2 (\mathbf{r}_0 \cdot \Phi \cdot \mathbf{r}_0) - (\Phi \cdot \mathbf{r}_0) \cdot (\Phi^2 \cdot \mathbf{r}_0), \\ t_2 &= (\Phi \cdot \mathbf{r}_0)^4 - (\Phi \cdot \mathbf{r}_0) \cdot (\Phi^2 \cdot \mathbf{r}_0) (\mathbf{r}_0 \cdot \Phi \cdot \mathbf{r}_0). \end{aligned} \right\} \quad (11)$$

If the solutions  $\lambda'$  and  $\lambda''$  of (10) are introduced in (9), the vectors  $\mathbf{v}$  and  $\mathbf{w}$  are obtained:

$$\mathbf{v} = \frac{\mathbf{r}_0 + \lambda' \Phi \cdot \mathbf{r}_0}{\pm |\mathbf{r}_0 + \lambda' \Phi \cdot \mathbf{r}_0|}, \quad \mathbf{w} = \frac{\mathbf{r}_0 + \lambda'' \Phi \cdot \mathbf{r}_0}{\pm |\mathbf{r}_0 + \lambda'' \Phi \cdot \mathbf{r}_0|}. \quad (12)$$

It has to be proved that

$$\mathbf{v} \cdot \mathbf{w} = 0. \quad (13)$$

The two equations (12) are introduced into (13):

$$1 + \lambda' \lambda'' (\Phi \cdot \mathbf{r}_0)^2 + (\lambda' + \lambda'') \mathbf{r}_0 \cdot \Phi \cdot \mathbf{r}_0 = 0. \quad (13')$$

But, from equation (10),

$$\lambda' \lambda'' = t_0/t_2, \quad \lambda' + \lambda'' = -t_1/t_2. \quad (14)$$

By introducing (14) in (13') and making use of (11), an identity is obtained. Hence, there is a 'triangle'  $UVW$  such that one of its vertices,  $U$ , is  $90^\circ$  away from  $P_0$ . If  $P_0$  is in a general position (not on a symmetry plane of the ellipsoid), it cannot be  $90^\circ$  away from any of the vertices of the 'true triangle'. Therefore,  $UVW$  is the 'ghost triangle'.

We are very grateful to our colleague H. Cortés for his valuable help in the mathematical part of this work, to our colleague C. Rivera for his keen participation in several useful discussions, and to G. Gifford and H. Villarroel for having drawn many of the projections which were required for § 2 of this work.

One of us (N. J.) has great pleasure in acknowledging the valuable advice of Dr W. A. Wooster, Dr N. F. M. Henry and Dr I. D. Muir of the Department of Mineralogy and Petrology, Cambridge University, in the final stages of the presentation of this paper, and is indebted to the British Council for a Research Scholarship under which this work was finished.

## References

- BERNAL, J. D. & CARLISLE, C. H. (1947). *J. Sci. Instrum.* **24**, 107.  
 JOEL, N. (1950). *Miner. Mag.* **29**, 206.  
 JOEL, N. (1951). *Miner. Mag.* **29**, 602.  
 PERUTZ, M. F. (1949). *J. Sci. Instrum.* **26**, 127.  
 PHEMISTER, T. C. (1954). *Amer. Min.* **39**, 172.  
 WILSON, E. B. (1943). *Vector Analysis*. New Haven: Yale University Press.  
 WRIGHT, F. E. (1923). *J. Opt. Soc. Amer.* **7**, 779.

*Acta Cryst.* (1957). **10**, 406

## The Structure of Potassium Pyrosulfite and the Nature of the Pyrosulfite Ion.

BY INGVAR LINDQVIST AND MAJ MÖRTSELL

*Institute of Chemistry, University of Uppsala, Uppsala, Sweden*

(Received 28 January 1957)

The crystal structure of  $K_2S_2O_5$  has been confirmed and refined by a least-squares method. The lattice constants are  $a = 6.936 \pm 0.005$ ,  $b = 6.166 \pm 0.008$ ,  $c = 7.548 \pm 0.006$  Å,  $\beta = 102^\circ 37' \pm 6'$ . The space group is  $P2_1/m$ , and  $Z = 2$ . The  $S_2O_5^{2-}$  ion can best be described as a thionite-thionate ion. The bond lengths are 2.209 Å (S-S), 1.499 Å (S-O in the thionite group) and 1.431 Å, 1.472 Å (S-O in the thionate group).

The experimentally determined bond angles have been used for an exact calculation of the sulphur hybrid orbitals, assuming that these are orthogonal combinations of 3s and 3p orbitals. The results prove that this assumption is correct for the thionate group, and indicate that the bond lengths are principally determined by the s character of the hybrid orbitals which form the  $\sigma$  bonds.

The crystal structure of potassium pyrosulfite,  $K_2S_2O_5$ , was determined by Zachariasen (1932). In the discussion of the structure the author emphasizes the fact that the structure obtained (with S-S bonds) is contrary to the formula given by the chemists (with S-O-S bonds) (cf. however a discussion by Hägg, 1932). Because of the importance of this result for theoretical chemistry we found it worth while to re-investigate the structure. This study has essentially confirmed the earlier results.

### Crystal data

A single crystal of the size  $0.3 \times 0.1 \times 0.07$  mm.<sup>3</sup> was enclosed in a capillary tube and used for the X-ray study. The unit cell has been redetermined, using a method first described by Weiss, Cochran & Cole (1948). Systematic errors were eliminated by a method of extrapolation worked out by Löfgren (1957).

The new results are (the old values within brackets):

$a = 6.936 \pm 0.005$  Å (6.95 Å),  $b = 6.166 \pm 0.008$  Å (6.19 Å),  $c = 7.548 \pm 0.006$  Å (7.55 Å) and  $\beta = 102^\circ 37' \pm 6'$  ( $102^\circ 41'$ ).

The space group is  $P2_1/m$  and  $Z = 2$ . The calculated density is 2.34 g.cm.<sup>-3</sup> (found 2.3 g.cm.<sup>-3</sup>).

Weissenberg photographs were taken with Cu  $K\alpha$  radiation around the [110] axis (five layer lines). The intensities were visually estimated, and relative  $|F|^2$  values were calculated, using Lu's (1943) curves.

### Refinement of the structure

A least-squares refinement of the suggested structure was made on IBM 704 by Dr D. Sayre. The final results obtained are:

	<i>x</i>	<i>y</i>	<i>z</i>	<i>B</i> (Å <sup>2</sup> )
K <sub>I</sub>	0.215	0.250	0.936	1.7
K <sub>II</sub>	0.639	0.250	0.673	1.2
S <sub>I</sub>	0.027	0.250	0.329	1.4
S <sub>II</sub>	0.702	0.250	0.238	1.1
O <sub>I</sub>	0.078	0.051	0.235	2.4
O <sub>II</sub>	0.632	0.053	0.314	2.5
O <sub>III</sub>	0.660	0.250	0.043	2.7

The reliability factor is 0.136. A table with the observed and calculated structure factors can be obtained from this Institute.

The individual temperature factors have reasonable values. The variations obtained for the three oxygen atoms cannot easily be interpreted, but are probably not significant. The difference between K<sub>I</sub> and K<sub>II</sub> can be explained by the fact that K<sub>II</sub> is more narrowly enclosed by oxygen atoms than K<sub>I</sub> (Table I, *vide infra*). It is quite natural that S<sub>II</sub> surrounded by three oxygen and one sulphur has a smaller *B* value than S<sub>I</sub>, which is surrounded by only two oxygen and one sulphur (Fig. 1, *vide infra*).

The standard deviations in the atomic positions calculated from the residuals of the least-squares refinement would give the following standard deviations in the bond lengths: 0.002 Å for S-S, 0.004 Å for S-O and K-O, and 0.008 Å for O-O. In the struc-